Kinetic Monte Carlo simulations of adatom island decay on Cu(111)

Mats I. Larsson*
Department of Engineering Sciences, Physics and Mathematics, Universitetsgatan 1, Karlstad University, S-65188 Karlstad, Sweden
(Received 30 January 2001; revised manuscript received 29 March 2001; published 31 August 2001)

Kinetic Monte Carlo simulations are used to investigate the recent scanning tunneling microscopy (STM) measurements of fast decaying adatom islands on Cu(111). First, reduced potential barriers for adatom migration along close-packed ⟨011⟩ step edges having {100} or {111} step risers are shown to be very important to obtain close-to-monotonic decay of the island top layer, in correspondence to STM measurements. The best correspondence is obtained for fully suppressed one-dimensional Ehrlich-Schwoebel barriers. Second, for encounters between steps in adjacent atomic layers it is demonstrated that a moderately reduced step-edge potential energy barrier for adatom crossing of these steps is sufficient to obtain correspondence between simulations and experiments provided that the step-edge diffusion is increased. The step-step-interaction-related activation energy for step-edge crossing is found to be significantly lower than what was previously reported. This work shows that concerted atomic motion is not necessary to explain the rapid top-island decay if the low-coordinated step-edge transition states are properly modeled. Moreover, no critical step-step distance larger than one atomic row, for which rapid top-island decay occurs, is obtained in the simulations. Furthermore, the simulations are interesting because they show that dramatic macroscopic effects can be generated by just small changes of the potential-energy barriers that are controlling the surface diffusion rates.

DOI: 10.1103/PhysRevB.64.115428 PACS number(s): 68.35.Bs, 02.70.Rr, 61.14.−x, 05.40.−a

I. INTRODUCTION

In this work rapid decay of islands on fcc(111) surfaces and Cu(111) surfaces in particular will be investigated. To understand the controlling mechanisms for island decay surface diffusion of islands will be considered to start with. This phenomenon has been studied both experimentally and theoretically. For example, diffusion of Ir clusters on Ir(111) was recently investigated by Wang and Ehrlich using field ion microscopy[1] and migration of Ag clusters on Ag(100) surfaces was measured with scanning tunneling microscopy (STM) by Wen *et al.*[2] It was shown that island diffusion can be accomplished with neither monomers (i.e., single adatoms) on the surface nor evaporation of atoms from the island.

Theoretically, island diffusion was recently studied by Bogicevic *et al.*[3] using kinetic Monte Carlo (KMC) simulations. In their simulations the effect of monomer diffusion around island boundaries was investigated. An analytical expression was derived that corresponds well to experimental results, e.g., for Cu on Cu(100) and Ag on Ag(100) as reported by Pai *et al.*[4] Moreover, the temperature and the island size dependence of the island diffusion constant also for Cu on Cu(100) was investigated with KMC methods by Heinonen *et al.*[5] They found that the scaling exponent for the size dependence decreases with increasing island size.

Evangelakis *et al.* have recently reported on the surface diffusion of Cu islands on flat Cu(111).[6] It is shown that the Cu island diffusion is mainly accomplished by fast step-edge diffusion of the boundary atoms in such a sense that a concerted motion of the whole island is achieved. To a minor extent also creation and annihilation of adatoms and vacancies contribute to the island migration, which is similar to the model reported for Ir on Ir(111).[1] The concerted island diffusion mechanism does not explain the one-dimensional (1D) island diffusion on fcc(110)-(1×2) surfaces. For this system a leapfrog diffusion mechanism was reported by Linderoth *et al.*[7] and by Montalenti and Ferrando[8] who used STM and molecular dynamics calculations, respectively. Leapfrog diffusion is a descriptive name for the mechanism where an atom terminating a linear chain of atoms detaches from one end of the chain, goes to the top and diffuses to the opposite end of the chain.

Not only the island diffusion is strongly dependent on the step-edge migration of adatoms but also the island shape. Generally, to obtain and to maintain compact islands, a strongly reduced potential barrier for atomic migration along step edges is a prerequisite. In detail how the adatom diffusion along island boundaries affects island shapes was investigated by Liu *et al.*[9] and Bartelt and Evans[10] using KMC simulations, and Hohage *et al.*[11] who presented results from both KMC simulations and STM measurements.

Theoretical calculations for Cu(111) point out that the potential energy barriers for step-edge diffusion along type *A* and *B* steps having {100} and {111} step risers, respectively, do not vary very much, according to Karimi *et al.*[12] But there is a small difference between the binding energies for atoms in *A* and *B* steps where the type *A* step is the most stable one, as reported by Breeman, Barkema, and Boerma,[13] resulting in hexagonal islands with longer *A*-steps than *B*-steps at least for low temperatures. But in the STM measurements[14,15] no preferred island edge orientation was observed to result in well-shaped hexagonal islands, which implies that the diffusion along Cu(111) steps should effectively have the same energy barrier for diffusion along both *A* and *B* steps, at least for the investigated temperature range. Nevertheless, in a recent paper[16] it is experimentally shown that the free step energy is 1% lower for *A* than for *B* steps. This study was performed for vicinal Cu(111) surfaces where the Cu islands nucleate on hcp rather than fcc sites. But on singular Cu(111) surfaces the Cu islands nucleate on fcc sites where the ratio between the free step energy for *A* and *B* steps is reversed,

i.e., type *B* steps are somewhat more favorable.[17] Giesen suggests the elastic strain field on vicinal surfaces, arising from the step structure, as the reason for this mechanism. The presence of stacking faults could probably also be important in this context. The problem of stacking faults during homoepitaxial growth of Cu on Cu(111) was recently discussed by Camarero *et al.*[18]

Because the temperature range studied in the present report coincides with the experimental one and the difference in step energy between the close-packed steps is so small it is not discriminated in the model between step-edge diffusion along the two close-packed step types.

Recently, the importance of the step-edge diffusion for the surface morphology evolution has been extensively studied, e.g., by Larsson,[19] who reported on a step-edge-diffusion–driven instability mechanism for step bunching. This mechanism was due to the introduction of a 1D ES barrier for step-edge diffusion at kink and corner sites. Thereafter the role of the 1D Ehrlich-Schwoebel (ES) barrier for the evolution of surface morphology has been studied, e.g., by using density-functional calculations by Bogicevic, Strömquist, and Lundqvist,[20] kinetic Monte Carlo simulation models by Ramana Murty and Cooper,[21] and discrete rate equations by Pierre-Louis, D'Orsogna, and Einstein.[22]

Azimuthal-dependent 2D ES barriers were discussed in a recent first-principles calculation of the ES barriers on Pt(111),[23] where Feibelman reports that the ES barrier of type *A* steps having {100} step risers are one order of magnitude smaller than the ES barrier for type *B* steps having {111} step risers. Furthermore, the ES barrier can be very much reduced by surfactants such as oxygen on Pt(111), as reported by Esch *et al.*[24] The effects of various potential-energy landscapes on the adatom diffusion across step edges, including the reduction of the ES barrier, was recently reported by Kyuno and Ehrlich.[25]

Another possible mechanism for crossing step edges is an exchange mechanism where the ascending or descending atom does not experience any ES barrier as discussed by Stumpf and Scheffler.[26] Li and DePristo,[27] and Giesen and Ibach,[28] proposed that this so called concerted atomic motion process is energetically the most favorable one for rapid island decay. This is supported by very recent *ab initio* calculations by Feibelman.[29]

Fast decay of adatom islands and mounds on Cu(111) was recently observed by Giesen, Schultze Icking-Konert and Ibach[14] by means of STM measurements. For this system a dramatic increase in the island decay rate was discovered when a small 2D island migrating on top of a larger one encounters the boundary of the larger island. The decay rate was found to be two orders of magnitude larger than for island layers keeping some distance between adjacent step edges. In a recent study[28] Giesen and Ibach propose that the potential-energy barrier for material transport across steps is reduced when the migrating top island encounters a descending step. According to this study, the reduction of atom detachment barriers from island step edges by approximately 0.1 eV rather than vanishing of step-edge barriers[30] can explain the results.

A second type of island decay was presented by Morgenstern *et al.*,[31] who analyzed the decay of Ag adatom and Ag vacancy islands situated approximately centered in a large hexagonal vacancy island. This was done in order to obtain the activation energies for hopping on a flat Ag(111) surface and the ES barrier.[32,33] Thereafter rapid top-island decay was also reported for Ag(111) in two recent publications.[34,35] Morgenstern *et al.*[35] supported Giesen and Ibach[28] that concerted motion is the most probable mechanism for the rapid island decay. Whether there is a critical separation between adjacent island step edges due to the quantum confinement effect is also still an open question.[28,35]

The intent of this paper is to use KMC simulations to study the dynamics of 2D Cu islands on Cu(111). In particular, the effect of step-step-interaction–induced reduction of the interlayer potential energy barriers will be investigated in conjunction with the influence of reduced potential barriers for step-edge diffusion along the island boundaries and 1D ES barriers for corner crossing. The effect of the 1D ES barrier in this context is difficult to model with rate equations, which motivates the use of KMC simulations.

II. KINETIC MONTE CARLO MODEL

The kinetic Monte Carlo model used in this work is a full-diffusion bond-counting model. It is a slightly modified version of the model described in Ref. 19. The hopping rate

$$\nu(n_i,n_f)=\nu_0\exp[-E(n_i,n_f)/kT] \tag{1}$$

is dependent on both the initial coordination number n_i (i.e., the number of nearest neighbors before a hop) and the final coordination number n_f (i.e., the number of nearest neighbors after a hop). Only adatom occupation of fcc lattice sites is modeled, which is the growth mode reported for singular Cu(111).[17] In this study the attempt frequency $\nu_0=3\times10^{12}\,\mathrm{s}^{-1}$ is tentatively chosen for an atomic hop in one of the six possible hop directions given by the hexagonal surface cell, presuming that there are no big differences among the attempt rates for various mechanisms. $E(n_i,n_f)$ is the coordination-number-dependent activation energy for surface diffusion, k is Boltzmann's constant and T is the substrate temperature. $\exp[-E(n_i,n_f)/kT]$ is related to the probability that one particular hop attempt will succeed. The potential-energy barrier height or synonymously the activation energy $E(n_i,n_f)$ is given by

$$E(n_i,n_f)=n_iE_0-(n_i+n_f)E_b, \tag{2}$$

where E_0 corresponds to the energy of an atomic bond, n_iE_0 is the binding energy for the initial site, and n_fE_0 is the binding energy for the final site. E_b is the barrier-height-tuning parameter and $-(n_i+n_f)E_b$ reduces the barrier compared to n_iE_0. The potential-energy landscape is schematically shown in Fig. 1. The potential-energy barrier $E(n_i,n_f)$ for a hop from site *i* to site *f* is marked with a double-headed arrow in the figure.

n_f is determined by counting the number of second-nearest neighbors (relative to the initial site) that will cause atomic bonds presuming that an atom hops to the final site. Thus, the second term on the right-hand side of Eq. (2) in-

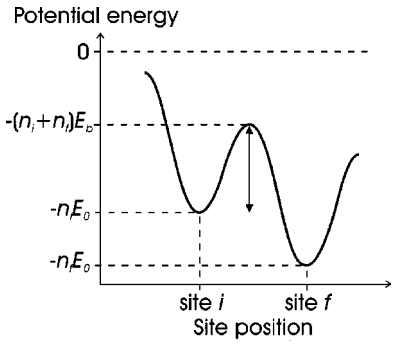

FIG. 1. Schematic potential-energy landscape showing the relationship between the energy parameters in the KMC model. The system is bound since the energy levels are negative. The activation energy for a hop from site *i* to site *f* is indicated with a double-pointed arrow.

cludes second-nearest-neighbor interactions, which was found in a recent work[19] to be important for a system to reach equilibrium effectively. The second-nearest-neighbor interaction gives the highest transition probability for a hop to the most highly coordinated site in the nearest neighborhood of an atom, i.e., the atoms probe their local surroundings for the most highly coordinated site. The second-nearest-neighbor interaction results in locally anisotropic surface diffusion if not all six coordination numbers n_f of the nearest-neighbor sites are equal, except for the case $E_b=0$ (when the diffusion always is locally isotropic). By using this form [Eq. (2)] for the activation energy the detailed balance is fulfilled, which is sufficient to obtain thermal equilibrium in a Monte Carlo simulation, according to Binder and Heermann.[36]

The (E_0,E_b) variables used in the KMC code should not be taken too literally but be regarded as help parameters to find the relevant potential-energy barriers that are the important parameters in the simulations. It may occur for certain (E_0,E_b) selections that some interactions give rise to negative activation energies. In reality, the activation energies $E(n_i,n_f)$ can never be negative, so accordingly these energies are set to zero in the program. Generally, for an interaction defined by $E(n_i,n_f)=E_1$ and $E(n_f,n_i)=E_2$ with $E_1 \geqslant 0$ and $E_2 \geqslant 0$ local (E_0,E_b) values describing that particular interaction can always be calculated by applying Eq. (2).

The energy parameters E_0 and E_b for various processes are determined using literature values. The average value for the nearest-neighbor bond energy, 0.37 eV, is reported for large clusters in Ref. 13. For smaller clusters the binding energy is reported to be larger,[13] obtaining its maximum value 0.44 eV for dimers. But the properties of very small clusters is not investigated in this study, which motivates the use of the binding energy $E_0=0.37$ eV in this work.

The potential-energy barrier can be adjusted by means of varying E_b. $E_b=0.17$ eV was derived for ''ordinary'' diffusion processes, which include all adatom migrating processes except step-edge diffusion and step-step-interaction–related mechanisms, i.e., the ''extraordinary'' processes. The most fundamental of the ''ordinary'' processes is probably monomer hopping on flat terraces. The activation-energy barrier for this process in the KMC model is $E_{\mathrm{dif}}=E(3,3)=0.09$ eV. This is easily checked by inserting $E_0=0.37$ eV, $E_b=0.17$ eV, $n_i=3$, and $n_f=3$ into Eq. (2). Papanicolaou and Evangelakis found for monomer diffusion on flat Cu(111) that two energy barriers are involved, one for low temperatures and one for high temperatures.[37] For the lower-temperature regime (80–300 K) 0.041 eV and for the higher temperatures (300–1000 K) 0.087 eV were found. The low-temperature value is in accord with measurements at further lower temperatures performed by Wulfhekel *et al.*[38] Hence, the activation energy used in the simulations corresponds well to the reported value, since the temperatures used here are in the range 300–500 K.

To further motivate the use of $E_0=0.37$ eV and $E_b=0.17$ eV for ''ordinary'' diffusion processes, the activation energy for adatom detachment from a sixfold coordinated kink site out onto the terrace is $E_{\mathrm{ad}}=E(6,3)=0.69$ eV that should be compared to the result of Ref. 39, i.e., $E_{\mathrm{ad}}+E_{\mathrm{dif}}=0.76\pm0.04$ eV. This corresponds well to the value 0.78 eV obtained for the KMC model with $E_{\mathrm{dif}}=0.09$ eV. Furthermore, it is shown later on in this section that the modeled activation energies correspond fairly well to the experimentally determined values for the 2D ES barriers.[15] An extended comparison between KMC-modeled activation energies and theoretical ones are presented in the Discussion section, where a reasonable correspondence is found. Thus, having shown that the model works well for the most important ''ordinary'' key diffusion processes, it is assumed to hold for the remaining ones. This approach is somewhat approximate; however, the set of potential barriers reported in the literature is incomplete and there are often large differences between values derived by various methods.

The next process considered is step-edge diffusion. Covered by the definition of step-edge diffusion in this work is surface diffusion along straight type *A* and *B* steps, including the corner sites with fourfold coordination connecting *A* and *B* step segments. It is shown in the next section that strongly enhanced step-edge diffusion is crucial to accurately simulate the experimental measurements. This is achieved in the simulations by increasing E_b. The various processes in step-edge diffusion are illustrated in Fig. 2 that shows a top view of a schematic hexagonal island, where the closed-shell island atoms are represented by black spheres and the step-edge diffusing atom situated on site 1 is represented by a gray sphere. For diffusion along the straight step edge, e.g., from site 1 to site 2, both the initial and the final coordination number is 5, giving the activation energy $E(5,5)=5E_0-10E_b$ for this process. This means that the activation energy is zero for $E_b=0.185$ eV. The potential-energy barrier for the atom to hop from site 2 to site 3 is higher $[E(5,4)=5E_0-9E_b]$, since the final coordination number in this case is 4. Thus, $E(5,4)$-$E(5,5)$ gives the 1D ES barrier because that is the difference in activation energy between the two involved processes. The 1D ES barrier is reduced to zero by selecting $E_b=0.206$ eV. Then there will be no activation energy at all for step-edge diffusion around the circumference of a perfect island, i.e., the hopping rate is given by the attempt frequency. Strictly speaking, the activation energy cannot vanish completely because than there is no separation

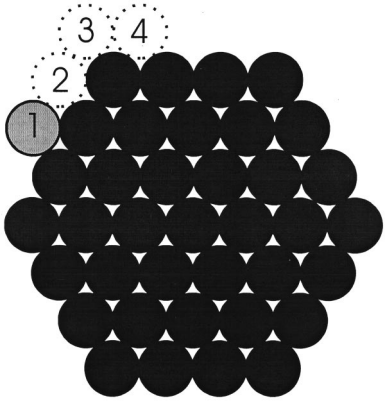

FIG. 2. Schematic top view of a hexagonal island, where the black spheres represent the closed-shell island atoms and the gray sphere represents an adatom situated at the step. The dashed circles denote sites involved in the various step-edge diffusion processes described in the text.

between the involved potential wells and there will be no rate. But in practice, it is possible to work with vanishing diffusion barriers since even if the barrier is not allowed to be smaller than some bias value δE, the resulting rate will only be reduced by a small fraction compared to its maximum value ν_0. For example, if $\delta E = 0.01$ eV the rate is just 20–30 % smaller than ν_0 for temperatures between 500 and 300 K.

For the step-edge diffusion process $E_b = 0.16$ eV was derived using the literature value 0.24 eV that is reported to be the upper limit for the $E(5,5)$-activation energy for step-edge diffusion along type A steps.[40] The prefactor for this process was reported to be $1.87 \times 10^{15\pm2}\ s^{-1}$. The activation energy 0.24 eV is found in the simulations to be too high (see below), resulting in an insufficiently low step-edge-diffusion rate to give well-shaped hexagonal islands. This is reasonable since the prefactor used in the simulations ($\nu_0 = 3 \times 10^{12}\ s^{-1}$) is much smaller than the experimental one. To find the most accurate step-edge diffusion rate, E_b is used as a fitting variable for these processes [i.e., $\nu(5,5)$, $\nu(5,4)$, and $\nu(4,5)$]. Note the E_b giving the overall best fit for the step-edge-diffusion processes is chosen and not one particular E_b value for each single process. The criteria used to find the most hexagonal shape is to minimize the number of kinks.

To find reasonable E_b values for the step-edge diffusion, simulations are performed. The outcome of these simulations is shown in Figs. 3(a) to 3(d). For each simulation 50 Mhops are executed. For the energies $E_b = 0.206$ and 0.185 eV the island shapes shown in the insets to Figs. 3(a) and 3(b), respectively, as well as the evolution of the number of kinks vs time plotted in Figs. 3(a) and 3(b) are very similar. The number of kinks fluctuates between 2 and 8 although also 0 and 10 are occasionally registered. The kinks are generated in pairs. Thereafter, the activation energy for step-edge diffusion was increased by using $E_b = 0.17$ and 0.16 eV in the simulations shown in Figs. 3(c) and 3(d), respectively. For

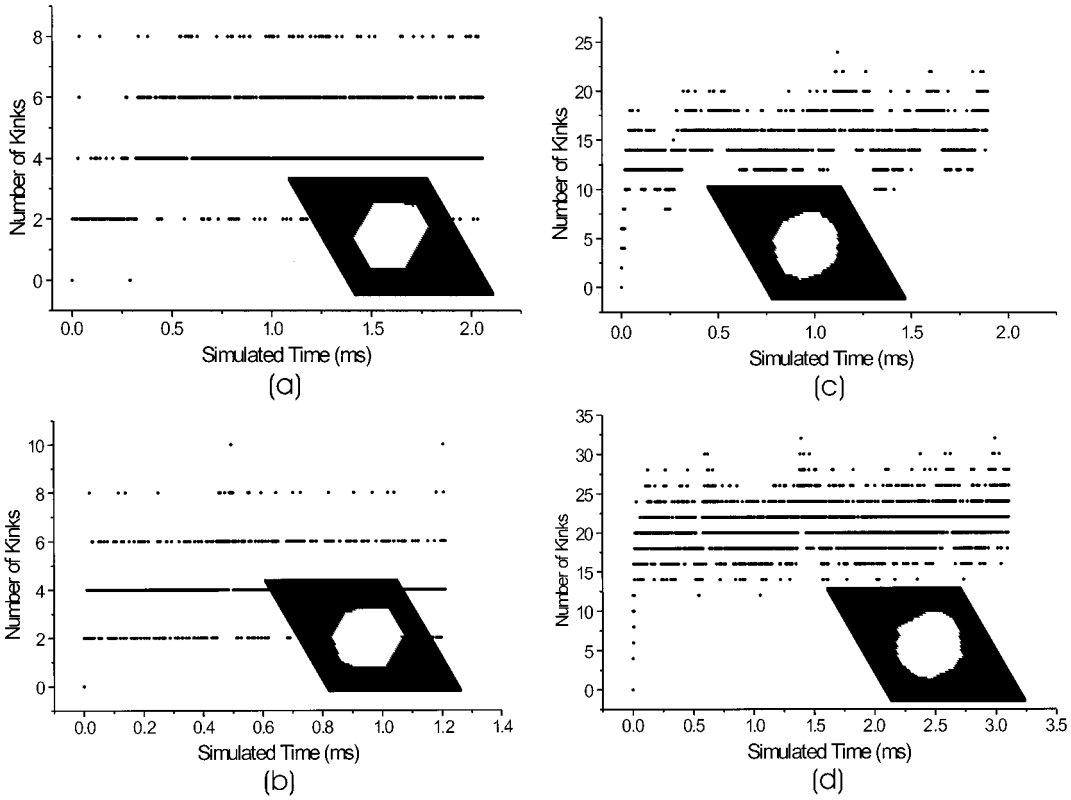

FIG. 3. Number of kinks vs time for various E_b values modeling the step-edge diffusion. The values are (a) $E_b = 0.206$ eV, (b) $E_b = 0.185$ eV, (c) $E_b = 0.17$ eV, and (d) $E_b = 0.16$ eV. The final island images after 50 Mhops are shown in the insets. $T = 423$ K is used in all the figures.

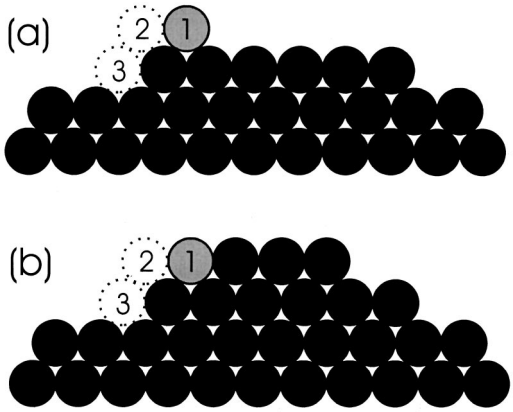

FIG. 4. Schematic cross-sectional side view of hexagonal islands with highly coordinated closed-shell atoms represented by black spheres and less coordinated adatoms occupying site 1 represented by gray spheres. The step-edge transition site is marked with 2 and the final site involved in the step-edge crossing with 3. (a) Ordinary step-edge crossing configuration with an Ehrlich-Schwoebel potential-energy barrier effectively reducing the adatom probability for crossing. (b) Step-step interaction step-edge crossing configuration, where a sufficiently reduced potential-energy barrier gives a high probability for adatom crossing.

these simulations, the island shape has become more rounded and the number of kinks has increased. The number of kinks fluctuates between 10 and 20 in Fig. 3(c) and between 14 and 28 in Fig. 3(d).

These results show that the number of kinks attains its minimum value for $E_b \geqslant 0.185\,\mathrm{eV}$, i.e., for zero activation energy for step-edge diffusion along straight type *A* and *B* steps [i.e., $\nu(5,5)$ processes]. Note there is still a 1D ES barrier for corner crossing for $E_b = 0.185\,\mathrm{eV}$ because $E(5,4) - E(5,5) = 0.185\,\mathrm{eV}$; however, for diffusion along straight steps the activation energy is zero with the hopping rate given by the attempt frequency. But for $E_b = 0.206\,\mathrm{eV}$ the 1D ES barrier is zero [i.e., $E(5,4) - E(5,5) = 0\,\mathrm{eV}$] and all step-edge diffusion rates are given by the attempt frequency, i.e., $\nu(5,5) = \nu(5,4) = \nu(4,5) = \nu_0$.

The STM-measured island shape becomes more rounded with higher temperature[41] than the simulated ones for $E_b \geqslant 0.185\,\mathrm{eV}$. The reason for the simulation approach of optimizing the straight-step segments is that the step-edge diffusion mechanism is not implemented for the $\nu(6,5)$ process that is very common on rounded islands. However, if we assume that the $\nu(6,5)$ process is included in the step-edge-diffusion modeling, $\nu(6,5)$ would be equal to ν_0 for $E_b = 0.206\,\mathrm{eV}$. This means that all step-edge diffusion rates would be given by the prefactor also for the rounded island. Hence, the simulation results obtained for hexagonal islands can be used to compare and understand experiments with enhanced diffusion along rounded step edges.

To finish this section step-edge crossing mechanisms will be considered. The 2D Ehrlich-Schwoebel effect is not very strong for Cu(111); however, it is not negligible for the temperatures used in this study. The sites involved in adatom step-edge crossing are shown in a cross-sectional side view in Fig. 4(a). The atom (gray sphere) under investigation is initially at the threefold coordinated site 1. If it hops to the transient site 2 it has two nearest neighbors in the *A* step and one nearest neighbor in the *B* step. The hopping rate from site 2 to site 3 [with the corresponding activation energies $E(2,5)$ for *A*-steps and $E(1,5)$ for *B*-steps] is given by the attempt frequency since the activation energy for this process is zero for the energy parameters used in this work. The coordination number is five for adatoms at site 3 for both straight *A* and *B* steps resulting in a much lower hopping rate back to site 2. The total activation energy for crossing an *A* step is accordingly $E(3,2) + E(2,5) = E(3,2)$ and the corresponding activation energy for crossing a *B* step is $E(3,1) + E(1,5) = E(3,1)$. The accurate position for the ES barrier is between sites 1 and 2, according to Stumpf and Scheffler[26] for Al(111). It is reasonable to assume this to hold also for Cu. The ES barrier is defined as the extra activation energy needed to cross a step edge in comparison to the activation energy required for hopping from a site to an adjacent one on a flat terrace. To model the Ehrlich-Schwoebel effect without step-step interaction, the ''ordinary'' energy parameters, i.e., $E_0 = 0.37\,\mathrm{eV}$ and $E_b = 0.17\,\mathrm{eV}$, are used in the simulations. These values give the ES barriers $E(3,2) - E(3,3) = 0.17\,\mathrm{eV}$ and $E(3,1) - E(3,3) = 0.34\,\mathrm{eV}$ for type *A* and *B* steps, respectively. This corresponds well to the *A*-step barrier $0.19 \pm 0.02\,\mathrm{eV}$ and the weighted average ES barrier 0.22 eV that was reported as an estimate for all possible crossing processes for both *A* and *B* steps.[15] It is reasonable that the weighted average is closer to the *A* than the *B* step barrier since *A* step crossing has a higher rate than *B* step crossing.

The potential-energy barriers for step crossing are reduced when the top island encounters the edge of the lower one[14,28,30] To model this mechanism the configuration in Fig. 4(b) is considered, where a side view in cross section of a bilayer high island on a fcc substrate is shown. At the straight step of the top layer an adatom (gray sphere) is situated at site 1. The mean activation energy E_{rap} derived from STM measurements in Ref. 28 for the site 1 to site 3 transition is $E_{\mathrm{rap}} = 0.69 \pm 0.04\,\mathrm{eV}$. This implies for the KMC model that $E_b = 0.18\,\mathrm{eV}$ should be used for the step-step interaction processes; however, it is shown in the next section that the best correspondence between KMC simulations and experiments is obtained for a lower E_{rap}.

To summarize this section so far, there are six adjustable parameters in the model including the temperature. Of these, the atomic bond energy E_0, the ordinary barrier height tuning parameter E_b, and the prefactor ν_0 will be assigned the same values in all simulations in the following section. Only two energy parameters will be varied to find the optimal correspondence to the experiments. These parameters are the step-step interaction E_b and the step-edge diffusion E_b.

The rate selection and search procedures that are used in this work are thoroughly discussed in Refs. 19, 42 and 43. All simulations are performed on lattices of size 64×64 sites. The initial surface morphology used in all the simulations is shown in the lower inset to Fig. 5(a). It consists of a perfect fcc(111) surface on which there is an island consisting of two perfect hexagonal atomic layers centered on top of each other. The bottom layer has the size of 850 atoms and the top layer has the size of 660 atoms. Note, the simulations

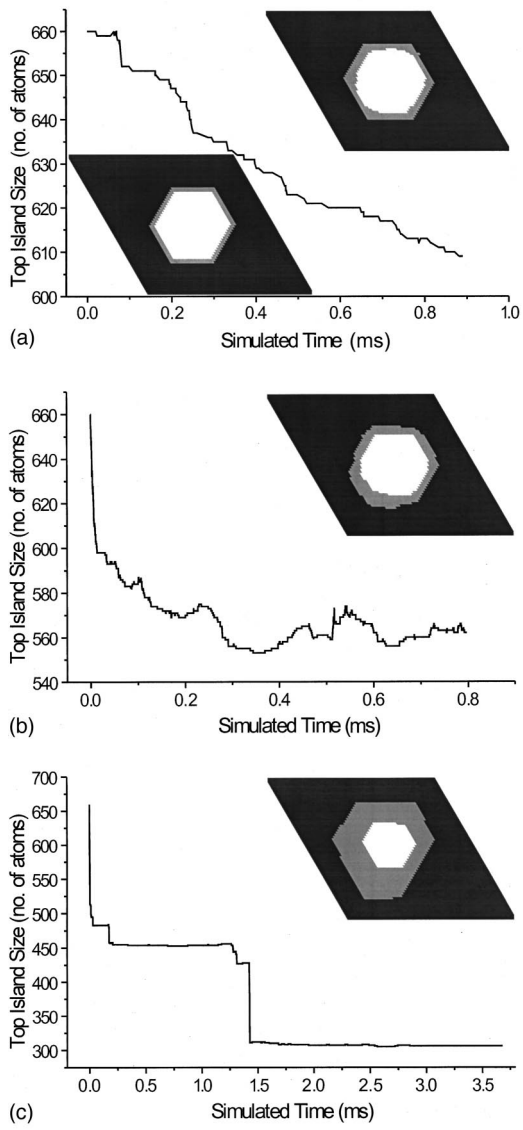

FIG. 5. Top-island decay vs time with the final surface image shown in the upper inset. The simulations shown in (a)–(c) are performed primarily to study the importance of the enhanced step-edge diffusion. The parameters used in the simulations are: (a) Step-step interaction $E_b=0.31$ eV, step-edge diffusion $E_b=0.185$ eV, $T=314$ K, and 200 Mhops. The initial surface is shown in the lower inset. (b) Step-step interaction $E_b=0.31$ eV, step-edge diffusion $E_b=0.185$ eV, $T=423$ K, and 100 Mhops. (c) Step-step interaction $E_b=0.31$ eV, step-edge diffusion $E_b=0.206$ eV, $T=423$ K, and 200 Mhops.

presented in this work are the representative ones that are picked out from a large set of calculations performed for different random-number sequences.

III. RESULTS

In this section the top-island decay will be simulated and compared to experimental results. This can be accomplished by studying the time dependence of the top-island size. The amplitudes of the fluctuations in the experimental decay curves are approximately 3% of the initial top-island size and long-term fluctuations as well as abrupt decays of the order of 10% or more of the initial top-island size are very uncommon. Simulated top-island decay curves deviating from the experimental characteristics will be rejected as unphysical.

It is not surprising that strong fluctuations are not observed in experiment since the gradient in the chemical potential causes a net downhill flux, which is observed as permanent island decay on the macroscopic time scale of a STM experiment. The gradient in the chemical potential and the net downhill flux vanish when the system reaches thermal equilibrium. That is, in the thermodynamic limit the decay of the inner island has to be monotonic: an increase in the area of the inner island would correspond to an increase in the free energy of the system. But there are other material systems where the thermal equilibrium configuration consists of multilayer islands due to quantum confinement effects as reported by Yeh *et al.*[44]

In the KMC model the system can be driven into equilibrium in much the same way as in reality by correctly selecting the potential energy barriers for the involved atomic hopping processes, thereby obtaining very similar results by atomistic modeling as can be obtained by statistical physics.

In the rest of this section simulations using various sets of activation energies will be discussed. First, the effect of the step-edge diffusion mechanism and in particular the 1D ES barrier, and second, the best choice of activation energy for the step-step interaction mechanism will be investigated.

The step-edge diffusion will be demonstrated and discussed in connection with Figs. 5(a)–5(c). The simulations are performed using the energy parameters that are discussed in the previous section to give the best correspondence to experiments. That is, the bond energy $E_0=0.37$ eV and $E_b=0.17$ eV for all ''ordinary'' processes, i.e., except for step-step interaction between adjacent straight steps and step-edge diffusion. For the step-step interaction, $E_b=0.31$ eV is used to start with giving the activation energy zero for these processes. For step-edge diffusion $E_b=0.185$ eV is initially used. The temperature is 314 K and totally 200 Mhops are carried out in this simulation. The resulting surface image is shown in the upper inset to Fig. 5(a). Both the top and the bottom island layers are hexagonal. The corresponding top layer decay vs time is also shown in Fig. 5(a). The decay is close to monotonic in agreement with experimental decay curves.[14,30] The abrupt jumps in the decay curve are caused by rapid decay events of the top island. The corresponding step-edge diffusion energies for $E_b=0.185$ eV are $E(5,5)=0$, $E(5,4)=0.185$ eV, and $E(4,5)=0$.

Experimentally, island decay is measured up to the temperatures around 500 K.[14] The next step in this study is to increase the temperature to 423 K and to keep the other parameters fixed. The resulting surface after 100 Mhops is shown in the inset to Fig. 5(b). It is evident that in spite of the hexagonal island shape the top-layer decay is very non-monotonic. The fact, that almost monotonic decay is obtained for the temperature 314 K but not for 423 K can most likely be explained by freeze-out of atomic diffusion processes with highly coordinated initial states at low temperature.[20] To improve the top island decay characteristics the 1D ES barrier is tentatively eliminated by using E_b

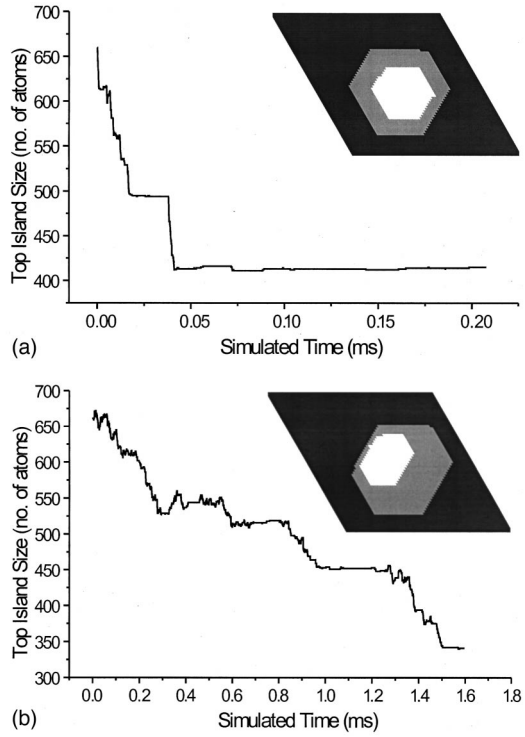

FIG. 6. Top-island decay vs time with the final surface morphology shown in the insets. The simulations shown in (a) and (b) are performed primarily to study the importance of the step-step-interaction mechanism. The parameters used in the simulations are (a) Step-step interaction $E_b=0.24$ eV, step-edge diffusion $E_b=0.206$ eV, $T=423$ K, and 100 Mhops; (b) step-step interaction $E_b=0.22$ eV, step-edge diffusion $E_b=0.206$ eV, $T=423$ K, and 100 Mhops.

$=0.206$ eV for the step-edge diffusion processes. This result is presented in Fig. 5(c). The top layer decay is almost monotonic indicating that the 1D ES barrier has a dramatic effect on the decay process. The short-term fluctuations are very weak for this temperature; however, there are very large abrupt top-island decays, proposing that the step-step-interaction–assisted step crossing is too efficient. The island shapes are hexagonal with just a few kinks at the step edges. The surface image shown in the inset to Fig. 5(c) was generated after a total of 200 Mhops.

Next, the sensitivity of the step-step-interaction activation energy will be considered. In the simulations the breakpoint between smooth and rough top-island decay was found for the step-step interaction E_b in the interval $0.22<E_b<0.24$ eV. In Figs. 6(a) and 6(b) representative results are shown for simulations using $E_b=0.24$ and 0.22 eV, respectively. The step-edge diffusion is modeled by $E_b=0.206$ eV (i.e., for fully suppressed 1D ES barriers) and $T=423$ K in both simulations. It is obvious that the decay curve is much smoother in Fig. 6(a) than in Fig. 6(b) although it shows some large abrupt decreases in the top island size. These abrupt drops in top-island size are also obtained for $T=500$ K and to some extent even for $T=314$ K, which indicates that the step-step-interaction potential-energy barrier is too low. The island decay in Fig. 6(b) is somewhat rough with many temporary top-layer size fluctuations, although there is a slow long-term decay. The amplitudes of the fluctuations correspond to approximately 20 top-layer atoms, which is 3% of the initial top-layer size. Furthermore, there are no long-term fluctuations in the simulated decay curve, which is consistent with the experiments. The surface images are generated after 100 Mhops at the end of the simulations and shown as insets to the figures. The images are well-shaped hexagons with a few kinks each, which is expected for the used activation energies. Nevertheless, in simulations performed for step-step interaction $E_b=0.22$ eV and $T=500$ K the top-island decay commences to show weak long-term fluctuations, which indicates that the corresponding energy barrier could be too high. Thus a reasonable value is $E_b=0.23$ eV and a mean step-step-interaction potential-energy barrier of 0.36 eV results. This is half of the mean value 0.69 ± 0.04 eV reported in Ref. 28. A reason for this discrepancy is not obvious.

Representative simulations using the best-fit energy parameters, i.e., the step-step interaction $E_b=0.23$ eV and the step-edge-diffusion $E_b=0.206$ eV, are shown in Figs. 7(a)–7(c). The simulations are performed for the temperatures 300, 400, and 500 K. The top island decay in the figures is a little bit rough with many small temporary top-layer size fluctuations, although there is a slow long-term decay. The size of the fluctuation amplitude is approximately 20 top-layer atoms for 500 K, 10 atoms for 400 K, and only a few atoms for 300 K. Hence, the fluctuation amplitude corresponds to 3% of the initial top-layer size for 500 K and less than 1% for 300 K. Furthermore, there are neither large abrupt drops nor long-term fluctuations in the simulated decay curves, which is consistent with the experiments. The surface images shown as insets to Figs. 7(a)–7(c) are generated after 500, 200, and 100 Mhops, out of the totals of 1000, 400, and 200 Mhops, respectively. Both top and bottom islands are well-shaped hexagons with a few kinks each, which is expected for the used activation energies. The figures show clearly that it is not only the top islands that diffuse around; the larger bottom islands are also mobile. This effect is most obvious at high temperatures.

The best-fit mean step-step-interaction potential-energy barrier in the KMC simulation is very close to the mean (not weighted) activation energy 0.34 eV for a threefold coordinated monomer to cross a step in the simulations. But if the activation energy for the ''ordinary'' monomer step-edge crossing process coincides with the activation energy for the step-step interaction step-edge crossing process, why is the rapid top-layer decay observed at all? This is so because before a monomer can cross a step it has to detach from the top-island step with the activation energy 0.49 or 0.69 eV depending on whether the initial site is fivefold or sixfold coordinated. Second, the monomer has to avoid immediately attaching to the top-island step again. The reattachment rate is very high since in this case the initial site is threefold and the final site is sixfold or fivefold coordinated, which in both cases give the maximum rate for hopping back to the step. If the monomer finally manages to reach the step edge of the second layer, the mean activation energy to cross the step is 0.34 eV. Effectively, higher activation energy for monomer

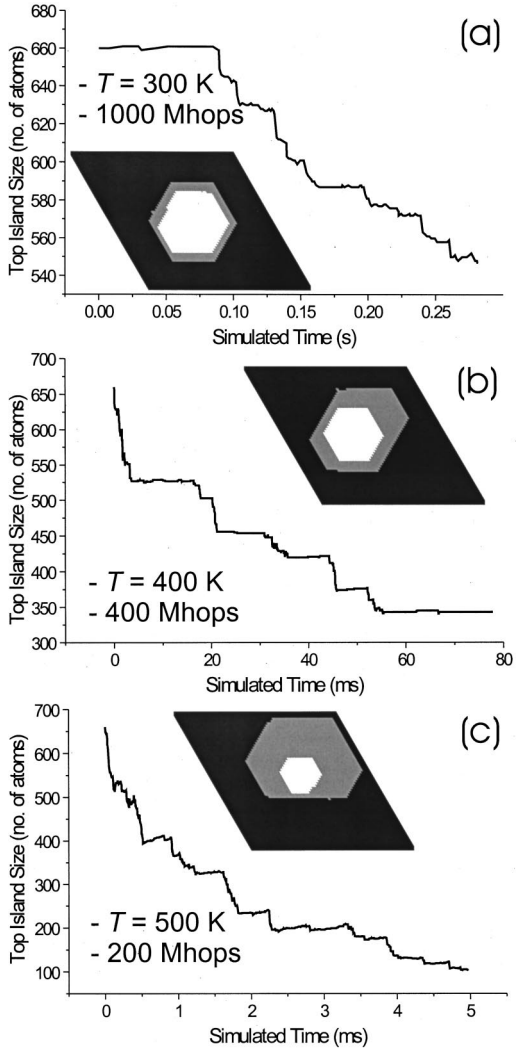

FIG. 7. Top-island decay vs time. Step-step interaction $E_b = 0.23$ eV and step-edge diffusion $E_b = 0.206$ eV are used in these simulations. Specific parameters are: (a) $T = 300$ K and 1000 Mhops, (b) $T = 400$ K and 400 Mhops, and (c) $T = 500$ K and 200 Mhops. The surface morphologies shown in the insets are generated after 500, 200, and 100 Mhops for figures (a), (b), and (c), respectively.

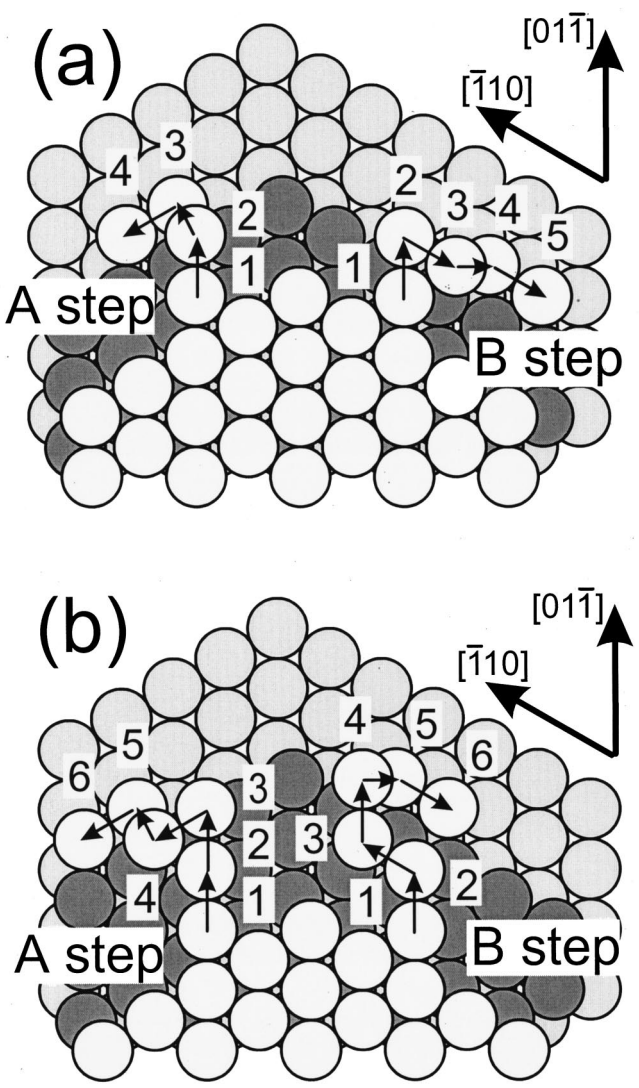

FIG. 8. Top-view surface morphologies showing step-step-interaction configurations in (a) and configurations with two intermediate atomic rows between adjacent steps in (b). The best-fit activation energies in the KMC simulations are presented below with the corresponding atomic hop within brackets. (a) *A*-step path: $E(5,2) = 0.24$ eV,$(1\rightarrow 2)$; $E(2,5) = 0$ eV,$(2\rightarrow 3)$; $E(5,5) = 0$ eV, $(3\rightarrow 4)$. *B*-step path: $E(5,1) = 0.47$ eV,$(1\rightarrow 2)$; $E(1,1) = 0.03$ eV, $(2\rightarrow 3)$; $E(1,5) = 0$ eV,$(3\rightarrow 4)$; $E(5,5) = 0$ eV,$(4\rightarrow 5)$. (b) *A*-step path: $E(5,3) = 0.49$ eV,$(1\rightarrow 2)$; $E(3,2) = 0.26$ eV,$(2\rightarrow 3)$; $E(2,2) = 0.06$ eV,$(3\rightarrow 4)$; $E(2,5) = 0$ eV,$(4\rightarrow 5)$; $E(5,5) = 0$ eV,$(5\rightarrow 6)$. *B*-step path: $E(5,3) = 0.49$ eV,$(1\rightarrow 2)$; $E(3,3) = 0.09$ eV,$(2\rightarrow 3)$; $E(3,1) = 0.43$ eV,$(3\rightarrow 4)$; $E(1,5) = 0$ eV,$(4\rightarrow 5)$; $E(5,5) = 0$ eV, $(5\rightarrow 6)$.

crossing of step edges than for step-step-interaction-assisted crossing of step edges is achieved.

IV. DISCUSSION

In this work it is shown that simple adatom hopping over step edges can qualitatively explain the STM observations of rapid top-island decay. Hence an interesting question is why the most common explanation for rapid island decay is a concerted motion mechanism of atoms at the step edge.[27–29] In the simulation step-edge crossing by hopping is considered. The involved processes are shown in Fig. 8(a), where the shortest path is used between the *A* steps, but not between the *B* steps. For the *A* step, the best-fit activation energies are $E(5,2) = 0.24$ eV and $E(2,5) = 0$ eV. The effective activation energy for the shortest path to cross the *A* step is $E^A(n_i, n_t, n_f) = E(n_i, n_t) + E(n_t, n_f)$, where n_t is the coordination number for the transition state, and $E^A(5,2,5) = 0.24$ eV follows. Similarly for the *B* step, the best-fit activation energies are $E(5,1) = 0.47$ eV, $E(1,1) = 0.03$ eV, and $E(1,5) = 0$ eV. For the shortest path to cross the *B* step, the activation energy is $E^B(5,1,5) = 0.47$ eV. These results are compared to corresponding theoretical literature values (the step type is denoted by a superscript if it is specified): $E^B(5,1,5) = 0.38$ eV (Ref. 45; concerted motion), $E^B(5,1,5)$

$=1.0$ eV (Ref. 29; hopping), and $E^A(5,2,5)=0.73$ eV (Ref. 45; concerted motion). No reported value for $E(1,1)$ could be found in the literature. It is generally reported that hopping has higher activation energies than the corresponding concerted motion processes. Why the activation energy for hopping over step edges becomes so high in the calculations is difficult to understand based on the KMC simulations; however, one possible suggestion is that the step-edge transition states are inaccurately taken into account in the models. As a matter of fact, it was found at an early stage of this work, that without including the transition states in the KMC model rapid island decay could not be obtained, unless the detailed balance condition was violated.

Furthermore, rapid diffusion along step edges is found to be crucial for the rapid island decay in this investigation. To achieve sufficiently high diffusion rates for the step running the corresponding activation energies used in this work are lower than reported in the literature.[12,40,45] These processes are also marked in Fig. 8(a). In the simulations the best fit to experimental top-island decay characteristics is obtained for $E(5,5)=0$ eV for both *A*- and *B*-steps. Representative calculated step-running barriers are $E(5,5)=0.228$ eV,[46] $E^A(5,5)=0.225$ eV,[45] $E^B(5,5)=0.325$ eV,[45] and $E^B(5,5)=0.29$ eV.[12] To explain the large difference between the best-fit KMC energies and the calculated ones the Meyer-Neldel rule[47] could tentatively be applied if it is assumed that the effective prefactor for step running differs significantly from the one used in the simulations. This is reported to be the case in Ref. 40 and is discussed in the KMC model section above. The Meyer-Neldel rule states that large activation energy is compensated by a large attempt frequency.

A second problem under investigation is whether a critical step-edge separation w_c exists or not, within which rapid island decay occurs. w_c is proposed to be caused by the quantum confinement effect. This hypothetical mechanism has been discussed for both Cu(111) and Ag(111).[28,35] To address this question in the framework of the present KMC model, a surface with one intermediate atomic row between the step edges of both *A*- and *B*-steps will be considered [see Fig. 8(b)]. The best-fit activation energies involved in the simulations for the *A* step path are $E(5,3)=0.49$ eV, $E(3,2)=0.26$ eV, $E(2,2)=0.06$ eV, $E(2,5)=0$ eV, and $E(5,5)=0$ eV, and for the *B*-step path the following activation energies are applied: $E(5,3)=0.49$ eV, $E(3,3)=0.09$ eV, $E(3,1)=0.43$ eV, $E(1,5)=0$ eV, and $E(5,5)=0$ eV. Some theoretical values are picked out to compare to the KMC simulation values: $E^B(5,3)=0.67$ eV (Ref. 12) and $E(5,3)=0.53$ eV.[6] The flat terrace $E(3,3)$ energy ranges from 0.028 to 0.094 eV (Refs. 12, 45, 37, 46) depending on calculation method and temperature. The step-edge-crossing activation energies are $E=0.365$ eV (Ref. 46) (step type unspecified) and $E^B(3,1,5)=0.49$ eV.[12] No literature value for $E(2,2)$ could be found. There are more activation energies presented in Refs. 12, 45, 46, e.g., for adatoms emitted out of various kink configurations, with which the best-fit KMC activation energies were compared. Generally a fairly good correspondence was found.

However, for these activation energies no rapid island decay can be obtained in the simulations independent of the number of intermediate atomic rows between adjacent step edges. It is obvious that adatom detachment from the top island is energetically the most critical process followed by the energy barriers for the step-crossing transition. Using a KMC model approach it is in principle possible to reduce the critical activation energies within a certain critical step-edge distance w_c to investigate whether an increased top-island decay rate can be obtained or not. Hence, if appropriate activation energies are chosen and the KMC code is accurately modified the existence of w_c cannot be excluded; however, this investigation is left for a future study.

It remains to discuss the different time scales in the experiments and the simulations. First, the experimental times for complete decay τ_{decay} will be reviewed and second, the large difference in decay times between simulations and experiments will be justified. The copper islands under investigation consist of a top layer with N_{top} atoms and a second layer with N_{low} atoms. Three STM experiments performed for various temperatures are picked out with the following parameters. (i) $N_{\text{top}}=5\times10^3$, $N_{\text{low}}=8\times10^3$, $T=314$ K, $\tau_{\text{decay}}=6\times10^3$ s,[28] (ii) $N_{\text{top}}=7\times10^3$, $N_{\text{low}}=15\times10^3$, $T=345$ K, $\tau_{\text{decay}}=3\times10^3$ s,[15] and (iii) $N_{\text{top}}=7\times10^3$, $N_{\text{low}}=23\times10^3$, $T=382$ K, $\tau_{\text{decay}}=2\times10^2$ s.[15] The corresponding parameters for the simulation are $N_{\text{top}}=650$, $N_{\text{low}}=850$, $T=423$ K, $\tau_{\text{decay}}=3\times10^{-3}$ s. Thus, a difference of five orders of magnitude in the decay time needs explanation.

The top islands in the experiment are one order of magnitude larger than in the simulation, which slows down the top-island decay considerably. It is reported in the literature[3,4] that the island diffusion constant $D\sim N^{-\gamma}$, where N is the number of island atoms and γ is 1.25 for Cu islands on Cu(100). Tentatively using this value also for Cu islands on Cu(111) another time increase factor of roughly 20 can be deduced, i.e., the top islands in the experiment diffuse 20 times slower than in the simulation. In addition, the initial second layer size $N_{\text{low}}=23\times10^3$ in experiment (iii) above should be compared to $N_{\text{low}}=850$ that was used in the simulation, which causes a time increase factor of roughly 30. The initial geometry in the simulations is designed such that the top layer is centered on top of the bottom layer with just two atomic rows between the step edges of adjacent layers. This implies optimal conditions for rapid decay already at the beginning of the simulations. This geometrical aspect is assumed to bring a time increase factor of 2–3.

Finally, the accuracy in the value of the prefactor ν_0 used in the KMC simulations is not very high. In practice it only makes sense to discuss an effective overall value for the prefactor because the prefactor varies in general for different diffusion processes. The effective prefactor can in reality be one or two orders of magnitude smaller than the one used in the simulations, which gives another time increase factor of 10–100. Multiplying the time increase factors gives a total increase in time of roughly five orders of magnitude. Hence the simulated time corresponds fairly well to the experimental one.

V. CONCLUSIONS

Kinetic Monte Carlo simulations were used to model the recently observed rapid decay of Cu islands on

Cu(111).[14,15,28,40] Two processes are found to be of immense importance to understand the experiments.

The first process is enhanced step-edge diffusion. It is found that whether there is a 1D ES barrier for crossing island corners or not has a large impact on the outcome of the simulations. For the lowest temperatures investigated, i.e., 300 and 314 K, almost monotonic top-layer decay is accomplishable even with a 1D ES barrier, but for the higher temperatures studied, i.e, 423 and 500 K, it is not possible. For these temperatures the condition for monotonic top-layer decay is that the maximum hopping rate is used for all step-edge diffusion processes with fully suppressed 1D ES barriers.

The second important process for the rapid top-layer decay is the step-step interaction between encountering steps of the top and bottom layers of the island. This interaction is modeled by varying the activation energy to cross the step for an atom situated at the step edge accurately involving the transition states in the simulations. The simulated time dependence of the top-island decay is in accord with experiments for the modeled mean activation energy 0.36 eV. This can be compared to 0.69 eV that was derived from experimental data.[28]

It is shown in this work that simple adatom step-edge crossing suffices to describe rapid top-island decay; however, after all scientific reports in favor for the concerted motion mechanism, it should also play an important role for the rapid decay process.

*FAX: +1-650-7233044. Email address: mats.larsson@kau.se

[1] S. C. Wang and G. Ehrlich, Phys. Rev. Lett. **79**, 4234 (1997).
[2] J.-M. Wen, J. W. Evans, M. C. Bartelt, J. W. Burnett, and P. A. Thiel, Phys. Rev. Lett. **76**, 652 (1996).
[3] A. Bogicevic, S. Liu, J. Jacobsen, B. Lundqvist, and H. Metiu, Phys. Rev. B **57**, R9459 (1998).
[4] W. W. Pai, A. K. Swan, Z. Zhang, and J. F. Wendelken, Phys. Rev. Lett. **79**, 3210 (1997).
[5] J. Heinonen, I. Koponen, J. Merikoski, and T. Ala-Nissila, Phys. Rev. Lett. **82**, 2733 (1999).
[6] G. A. Evangelakis, E. Vamvakopoulos, D. Pantelios, and N. I. Papanicolaou, Surf. Sci. **425**, L393 (1999).
[7] T. Linderoth, S. Horch, L. Petersen, S. Helveg, E. Lægsgaard, I. Stensgaard, and F. Besenbacher, Phys. Rev. Lett. **82**, 1494 (1999).
[8] F. Montalenti and R. Ferrando, Phys. Rev. Lett. **82**, 1498 (1999).
[9] S. Liu, Z. Zhang, G. Comsa, and H. Metiu, Phys. Rev. Lett. **71**, 2967 (1993).
[10] M. C. Bartelt and J. W. Evans, Surf. Sci. **314**, L829 (1994).
[11] M. Hohage, M. Bott, M. Morgenstern, Z. Zhang, T. Michely, and G. Comsa, Phys. Rev. Lett. **76**, 2366 (1996).
[12] M. Karimi, T. Tomkowski, G. Vidali, and O. Biham, Phys. Rev. B **52**, 5364 (1995).
[13] M. Breeman, G. T. Barkema, and D. O. Boerma, Surf. Sci. **323**, 71 (1995).
[14] M. Giesen, G. Schulze Icking-Konert, and H. Ibach, Phys. Rev. Lett. **80**, 552 (1998).
[15] M. Giesen and H. Ibach, Surf. Sci. **431**, 109 (1999).
[16] G. Schultze Icking-Konert, M. Giesen, and H. Ibach, Phys. Rev. Lett. **83**, 3880 (1999).
[17] M. Giesen, Prog. Surf. Sci. (to be published).
[18] J. Camarero, J. de la Figuera, J. J. Miguel, R. Miranda, J. Álvarez, and S. Ferrer, Surf. Sci. **459**, 191 (2000).
[19] M. I. Larsson, Phys. Rev. B **56**, 15 157 (1997).
[20] A. Bogicevic, J. Strömquist, and B. I. Lundqvist, Phys. Rev. Lett. **81**, 637 (1998).
[21] M. V. Ramana Murty and B. H. Cooper, Phys. Rev. Lett. **83**, 352 (1999).
[22] O. Pierre-Louis, M. R. D'Orsogna, and T. L. Einstein, Phys. Rev. Lett. **82**, 3661 (1999).
[23] P. J. Feibelman, Phys. Rev. Lett. **81**, 168 (1998).
[24] S. Esch, M. Hohage, T. Michely, and G. Comsa, Phys. Rev. Lett. **72**, 518 (1994).
[25] K. Kyuno and G. Ehrlich, Surf. Sci. **394**, L179 (1997).
[26] R. Stumpf and M. Scheffler, Phys. Rev. Lett. **72**, 254 (1994).
[27] Y. Li and A. E. DePristo, Surf. Sci. **351**, 189 (1996).
[28] M. Giesen, H. Ibach, Surf. Sci. **464**, L697 (2000).
[29] P. J. Feibelman, Surf. Sci. **478**, L349 (2001).
[30] M. Giesen, G. Schultze Icking-Konert, H. Ibach, Phys. Rev. Lett. **82**, 3101 (1999).
[31] K. Morgenstern, G. Rosenfeld, E. Lægsgaard, F. Besenbacher, and G. Comsa, Phys. Rev. Lett. **80**, 556 (1998).
[32] G. Ehrlich and F. G. Hudda, J. Chem. Phys. **44**, 1039 (1966).
[33] R. L. Schwoebel and E. J. Shipsey, J. Appl. Phys. **37**, 3682 (1966).
[34] K. Morgenstern, G. Rosenfeld, G. Comsa, E. Lægsgaard, and F. Besenbacher, Phys. Rev. Lett. **85**, 468 (2000).
[35] K. Morgenstern, G. Rosenfeld, G. Comsa, M. R. Sørensen, B. Hammer, E. Lægsgaard, and F. Besenbacher, Phys. Rev. B **63**, 045412 (2001).
[36] K. Binder and D. W. Heermann, *Monte Carlo Simulation in Statistical Physics: An Introduction* (Springer Verlag, Berlin, 1997).
[37] N. I. Papanicolaou and G. A. Evangelakis, in *Surface Diffusion Atomistic and Collective Processes*, edited by M. C. Tringides, Vol. 360 of *NATO Advanced Science Series B: Physics* (Plenum Press, New York, 1997).
[38] W. Wulfhekel, N. N. Lipkin, J. Kliewer, G. Rosenfeld, L. C. Jorritsma, B. Poelsema, and G. Comsa, Surf. Sci. **348**, 227 (1996).
[39] G. Schulze Icking-Konert, M. Giesen and H. Ibach, Surf. Sci. **398**, 37 (1998).
[40] M. Giesen and G. Schulze Icking-Konert, Surf. Sci. **412/413**, 645 (1998).
[41] M. Giesen, C. Steimer, and H. Ibach, Surf. Sci. **471**, 80 (2001).
[42] P. A. Maksym, Semicond. Sci. Technol. **3**, 594 (1988).
[43] D. D. Vvedensky and S. Clarke, Surf. Sci. **225**, 373 (1990).
[44] V. Yeh, L. Berbil-Bautista, C. Z. Wang, K. M. Ho, and M. C. Tringides, Phys. Rev. Lett. **85**, 5158 (2000).
[45] D. C. Schlößer, K. Morgenstern, L. K. Verheij, G. Rosenfeld, F. Besenbacher, and G. Comsa, Surf. Sci. **465**, 19 (2000).
[46] P. Stoltze, J. Phys.: Condens. Matter **6**, 9495 (1994).
[47] W. Meyer and H. Neldel, Z. Tech. Phys. (Leipzig) **12**, 588 (1937).